CHM-1, a novel synthetic quinolone with potent and selective antimitotic antitumor activity against human hepatocellular carcinoma *in vitro* and *in vivo*

Shih-Wei Wang,[1] Shiow-Lin Pan,[1] Yu-Chun Huang,[1] Jih-Hwa Guh,[2] Po-Cheng Chiang,[2] Der-Yi Huang,[1] Sheng-Chu Kuo,[3] Kuo-Hsiung Lee,[4] and Che-Ming Teng[1]

[1]Pharmacological Institute and [2]School of Pharmacy, College of Medicine, National Taiwan University, Taipei, Taiwan; [3]Graduate Institute of Pharmaceutical Chemistry, China Medical University, Taichung, Taiwan; and [4]Natural Products Laboratory, School of Pharmacy, University of North Carolina, Chapel Hill, North Carolina

Abstract

Hepatocellular carcinoma is highly chemoresistant to currently available chemotherapeutic agents. In this study, 2′-fluoro-6,7-methylenedioxy-2-phenyl-4-quinolone (CHM-1), a synthetic 6,7-substituted 2-phenyl-4-quinolone, was identified as a potent and selective antitumor agent in human hepatocellular carcinoma. CHM-1 induced growth inhibition of HA22T, Hep3B, and HepG2 cells in a concentration-dependent manner but did not obviously impair the viability of normal cells at the IC_{50} for liver cancer cells. CHM-1-induced apoptosis was also characterized by immunofluorescence microscopy. CHM-1 interacted with tubulin at the colchicine-binding site, markedly inhibited tubulin polymerization both *in vitro* and *in vivo*, and disrupted microtubule organization. CHM-1 caused cell cycle arrest at G_2-M phase by activating Cdc2/cyclin B1 complex activity. CHM-1-induced cell death, activation of Cdc2 kinase activity, and elevation of MPM2 phosphoepitopes were profoundly attenuated by roscovitine, a specific cyclin-dependent kinase inhibitor. CHM-1 did not modulate the caspase cascade, and the pan-caspase-inhibitor z-VAD-fmk did not abolish CHM-1-induced cell death. However, CHM-1 induced the translocation of apoptosis-inducing factor (AIF) from mitochondria to the nucleus. Small interfering RNA targeting of AIF substantially attenuated CHM-1-induced AIF translocation. Importantly, CHM-1 inhibited tumor growth and prolonged the lifespan in mice inoculated with HA22T cells. In conclusion, we show that CHM-1 exhibits a novel antimitotic antitumor activity against human hepatocellular carcinoma both *in vitro* and *in vivo* via a caspase-independent pathway. CHM-1 is a promising chemotherapeutic agent worthy of further development into a clinical trial candidate for treating cancer, especially hepatocellular carcinoma. [Mol Cancer Ther 2008;7(2):350–60]

Introduction

Hepatocellular carcinoma ranks as one of the most common cancers in the world (1). In Taiwan, where the incidence of hepatocellular carcinoma is among the highest in the world, chronic infection with hepatitis B virus appears to account for at least 70% of hepatocellular carcinoma (2). The incidence of hepatocellular carcinoma is dramatically increasing in the United States and other developed countries most likely due to the increasing prevalence of hepatitis C (3). Unfortunately, most patients with hepatocellular carcinomas are not curable because extensive resection is not possible, there is massive liver dysfunction caused by cirrhosis, or the disease is not identified at an early stage. Systemic chemotherapy and chemoembolization are the remaining treatment options in advanced hepatocellular carcinoma (4). However, hepatocellular carcinoma is well known for its expression of the multidrug resistance gene and its poor response to currently available chemotherapeutic agents (5, 6). Therefore, innovations to explore effective chemotherapeutic agents for hepatocellular carcinoma are urgently needed.

Antimitotic agents interact in the tubulin/microtubule system and constitute a major class of anticancer drugs (7). Because microtubules play crucial roles in the regulation of the mitotic apparatus, disrupting microtubules can induce cell cycle arrest in M phase, consequentially triggering of signals for apoptosis. Known antimitotic agents generally fall into three distinct groups (8). Microtubule-stabilizing agents, which bind to fully formed microtubules and prevent the depolymerization of tubulin subunits, are presented by paclitaxel and the taxanes, the epothilones, and discodermolide. The other two groups function by binding to the tubulin dimer and inhibiting their polymerization into microtubules. The *Vinca* alkaloids, typified by vinblastine, vincristine, and vinorelbine, are one of these groups. Colchicine and colchicine-site binders define the third group of antimitotic agents. Both the taxanes and the *Vinca* alkaloids are widely used to treat various kinds of

Received 8/26/07; revised 10/26/07; accepted 11/9/07.

Grant support: National Science Council of the Republic of China grant NSC 92-2320-B-002-072 (C-M. Teng) and NIH grant CA17625 (K-H. Lee).

The costs of publication of this article were defrayed in part by the payment of page charges. This article must therefore be hereby marked *advertisement* in accordance with 18 U.S.C. Section 1734 solely to indicate this fact.

Requests for reprints: Che-Ming Teng, Pharmacological Institute, College of Medicine, National Taiwan University, No. 1, Jen-Ai Road, Section 1, Taipei, Taiwan. Phone: 886-2-2322-1742; Fax: 886-2-2322-1742. E-mail: cmteng@ntu.edu.tw

doi:10.1158/1535-7163.MCT-07-2000

human cancers, whereas colchicine-site binders are being vigorously pursued as potential new chemotherapeutic agents (9).

Quinolone derivatives are initially discovered as bacterial DNA gyrase inhibitors and thus developed as antibacterial agents with low side effects (10). Our previous work showed that 2-phenyl-4-quinolones exhibited promising cytotoxicity in a broad spectrum of human cancer cell lines and inhibited platelet aggregation (11–16). We also showed the 2-phenyl-4-quinolone series inhibited tubulin polymerization by binding to tubulin at the colchicine-binding site and was exerted as antimitotic agents (11–15). Recently, some 2-phenylpyrroloquinolin-4-ones were synthesized from the 2-phenyl-4-quinolone and have been shown to inhibit the growth of hepatocellular carcinoma both *in vitro* and *in vivo* (17). Notably, 2′-fluoro-6,7-methylenedioxy-2-phenyl-4-quinolone (CHM-1) has been identified from 6,7-substituted 2-phenyl-4-quinolone derivatives in our laboratory as an anti-invasive agent in hepatocellular carcinoma cells (18). We found that CHM-1 inhibited cell invasion via the down-regulation of MMP-9 in SK-Hep-1 cells. In this study, we investigated the antitumor activity of CHM-1 against hepatocellular carcinoma in both *in vitro* and *in vivo* assays and further elucidated the mechanism of CHM-1-induced effects in hepatocellular carcinoma cells.

Materials and Methods

Materials

CHM-1 was obtained from the Graduate Institute of Pharmaceutical Chemistry, School of Medicine, China Medical University. 3-(4,5-Dimethylthiazol-2-yl)-2,5-diphenyltetrazolium bromide (MTT), propidium iodide, anti-β-tubulin monoclonal antibody, anti-endonuclease G polyclonal antibody, FITC-conjugated secondary antibody, and other chemical agents were bought from Sigma Chemical. Antibody to anti-OxPhos complex IV and Mitotracker Red CMXRos were obtained from Molecular Probes. Antibodies to cyclin A, cyclin B1, Cdc2, and nucleolin were purchased from Santa Cruz Biotechnology. Antibodies to stathmin, phospho-Cdc2 (Tyr^{15}), phospho-Cdc2 (Thr^{161}), caspase-8, and caspase-9 were purchased from Cell Signaling Technologies. Antibody to caspase-3 was purchased from Imgenex. Antibodies to glyceraldehyde-3-phosphate dehydrogenase (GAPDH), cIAP1, cIAP2, XIAP, and survivin were purchased from Abcam. Antibodies to MAP4, caspase-6, and caspase-7 were purchased from BD Biosciences PharMingen. Antibody to MPM2 was purchased from Upstate Biotechnology.

Cell Culture

The human hepatocellular carcinoma cell lines Hep3B and HepG2 were obtained from the American Type Culture Collection and cultured in DMEM. The human hepatocellular carcinoma cell line HA22T was obtained from Culture Collection and Research Center and cultured in DMEM. MRC5 (American Type Culture Collection) was cultured in MEM. AML12 (American Type Culture Collection) was cultured in DMEM/F-12. All cells were maintained in humidified air containing 5% CO_2 at 37°C.

Cell Viability Assay

Cells were inoculated in 96-well plates at a density of 10^4 per well, and the percentage of cell survival was assessed using MTT colorimetric assay.

Apoptosis Detection

Terminal deoxynucleotidyl transferase–mediated dUTP nick end labeling immunofluorescence staining (Promega) and Cell Death ELISA^{PLUS} kit (Roche Molecular Biochemicals) were used to determine apoptosis.

Cell Cycle Analysis

The cell cycle distribution was determined using FACScan flow cytometric analysis by DNA staining with propidium iodide.

Immunocytochemistry and Confocal Microscopy

After treatment, cells were fixed with methanol, blocked with 3% bovine serum albumin, stained with anti-β-tubulin or apoptosis-inducing factor (AIF) monoclonal antibody, and then FITC-conjugated antimouse IgG antibody. Mitotracker Red CMXRos (100 nmol/L) was added to the culture medium at 37°C for 30 min to stain mitochondria before fixation. Nuclear staining was done with 4,6-diamidino-2-phenylindole. Cells were imaged with Leica TCS SP2 Spectral Confocal System.

In vitro Microtubule Assembly Assay

The CytoDYNAMIX ScreenTM3 kits was purchased from Cytoskeleton and used for the detection of polymerization of tubulin/microtubule.

In vivo Microtubule Assembly Assay

The cell lysate in which the cytosolic and cytoskeletal fractions containing soluble (s) and polymerized (p) tubulin, respectively, was separated by centrifugation, resolved by electrophoresis through SDS-PAGE, and immunoblotted with an antibody against β-tubulin.

Immunoprecipitation and Western Blot Analysis

Nuclear and mitochondrial fractionation were done as described previously (19). Total protein was determined and equal amounts of protein were separated by 10-15% SDS-PAGE and immunoblotted with specific primary antibodies. The signal detected using an enhanced chemiluminescence detection kit (Amersham). For immunoprecipitation studies, total protein was precipitated with anti-Cdc2 antibody and mixed overnight at 4°C. The following day, protein A/G^{PLUS}-agarose beads were added and incubated with gentle rocking at 4°C. Then, immunoblotting was done using anti–cyclin B1 antibody and anti-Cdc2 antibody.

Cdc2 Kinase Assay

A Cdk1/Cdc2 Kinase Assay Kit (Upstate Biotechnology) was used to determine the activity of Cdc2 kinase according to the manufacturer's instructions.

Measurement of Caspase Activity

The commercial assay kit (BioVision) was used to determine caspase activity.

RNA Interference

Stealth RNA interference targeting AIF mRNA was obtained from Invitrogen and used according to the

manufacturer's instructions. The AIF small interfering RNA (siRNA) sequence used was 5′-GGCCAGGGUACUGAUUGUAUCUGAA-3′, and the control siRNA, with no homology to any human mRNA, was 5′-GGCGGUGCAGUUAGUAUCUUACGAA-3′. For transfection, HA22T cells were seeded in 24-well plates or 10-cm dishes at 50% confluency with siRNA duplexes (200 nmol/L) using LipofectAMINE 2000 (Invitrogen). Following siRNA treatment, cells were treated with indicated agents for 24 h and then analyzed using Western blot analysis.

S.c. Xenograft Model

CHM-1 was dissolved completely in a vehicle mixture of DMSO/Cremophor EL/saline. As a comparison, the positive control doxorubicin was diluted with sterile saline before injection. Male severe combined immunodeficient mice (4-6 weeks of age), were purchased from the Laboratory Animal Center of the Medical College of National Taiwan University. HA22T cells (6×10^6) were injected s.c. into the flank of each animal. When tumors reached an approximate volume of 50 mm^3, mice were selected and distributed for drug studies. Tumor volumes were determined by measuring the length (l) and the width (w) and the volumes were calculated as $V = lw^2 / 2$. The mice were sacrificed and the tumors were excised after 1 month of treatment with CHM-1 and doxorubicin by i.p. injection twice weekly.

In vivo Antitumor Activity Assay

HA22T cells were injected i.p. at 10^7 per mouse into male severe combined immunodeficient mice on day 0; all drugs were delivered by i.p. against i.p. tumors on day 1. CHM-1 and doxorubicin were administrated twice weekly until doxorubicin-treated mice were all dying. The mice were observed daily and any deaths were recorded. Antitumor activity was assessed as the ratio of median survival time in the treatment group (T) to median survival time in the control group (C), and the results are shown as T/C: lifespan T/C (%) = [(median survival time of drug-treated group) / (median survival time of control group)] $\times$ 100.

Immunohistochemistry

Immunohistochemical studies were done on formalin-fixed, paraffin-embedded tumor tissues as described previously (20). The primary antibodies AIF (Cell Signaling Technologies) and MPM2 (Dako) were used in this study. A standard labeled streptavidin-biotin technique (Dako) was used to detect the reaction products.

Statistical Analyses

Data are presented as the mean $\pm$ SE for the indicated number of separate experiment. Statistical analyses of data were done with one-way ANOVA followed by Student's t test, and P values less than 0.05 were considered significant.

Results

CHM-1 Induces Growth Inhibition and Apoptosis via G_2-M-Phase Arrest in Human Hepatocellular Carcinoma Cells

We first determined the effect of CHM-1 on the growth of hepatocellular carcinoma cell lines using the MTT assay. CHM-1 induced significant concentration-dependent growth inhibition in HA22T, Hep3B, and HepG2 cells, with the most potent effects observed in HA22T cells (IC_{50}, 0.75 $\pm$ 0.11 μmol/L; Fig. 1B, *left*). Importantly, CHM-1 was less toxic to normal cell types, including human fibroblasts (MRC5) and mouse hepatocytes (AML12; Fig. 1B, *right*). These data indicate that CHM-1 induces selective cytotoxicity in human hepatocellular carcinoma cells but less in normal cells. CHM-1 caused the accumulation of G_2-M phase with concomitant losses in G_0-G_1 phase, with a maximum effect observed at 24 h (Fig. 1C). The accumulation of cells with G_2-M DNA content was followed by an increase in hypodiploid cells at the later time points (48 h) as indicated as apoptotic cells. The terminal deoxynucleotidyl transferase–mediated dUTP nick end labeling assay and quantitative assessment of oligonucleosomal DNA fragmentation were then used to identify apoptotic cell death. CHM-1 induced cell apoptosis with positive terminal deoxynucleotidyl transferase–mediated dUTP nick end labeling reactions in HA22T cells (Fig. 1D, *left*). After 24- and 48-h treatment, CHM-1 caused apoptotic cell death in a concentration-dependent manner (Fig. 1D, *right*). These results indicate that CHM-1 induced G_2-M arrest of the cell cycle followed by apoptosis.

CHM-1 Inhibits the Polymerization of Microtubules

As shown in Fig. 2A, the microtubule network exhibited normal arrangement and organization in HA22T cells in the absence of drug treatment. CHM-1 treatment caused changes in microtubule distribution starting with a 4-h exposure, and treatment with CHM-1 for 24 h resulted in findings similar to those of colchicine-induced microtubule changes. Colchicine and vincristine caused cellular microtubule depolymerization with short microtubule fragments scattered throughout cytoplasm. Paclitaxel resulted in microtubule polymerization with an increase in the density of cellular microtubules. In *in vitro* microtubule assembly assay, CHM-1 inhibited tubulin polymerization in a concentration-dependent manner (Fig. 2B). For comparison, tubulin polymerization was significantly promoted by paclitaxel and completely inhibited by vincristine. The effect of CHM-1 on microtubule assembly was compared with that of colchicine, paclitaxel, and vincristine in *in vivo* assays. After cells were treated with various antimitotic agents for 24 h, CHM-1, colchicine, and vincristine caused inhibition of microtubule assembly (Fig. 2C). In contrast, paclitaxel induced dramatic promotion of tubulin polymerization. The percentage of polymerized tubulin levels was 40.5 $\pm$ 2.0% for control samples and 20.8 $\pm$ 6.2%, 22.2 $\pm$ 5.8%, 57.1 $\pm$ 1.4%, and 36.2 $\pm$ 1.2% for treatment with CHM-1, colchicine, paclitaxel, and vincristine, respectively. Stathmin is a major microtubule-destabilizing protein that promotes microtubule depolymerization, and MAP4 is a microtubule-associated protein that stabilizes microtubules (21). In the present study, CHM-1 (1-10 μmol/L) did not affect the expression of stathmin but induced a concentration-dependent inhibition of MAP4 expression (Fig. 2D).

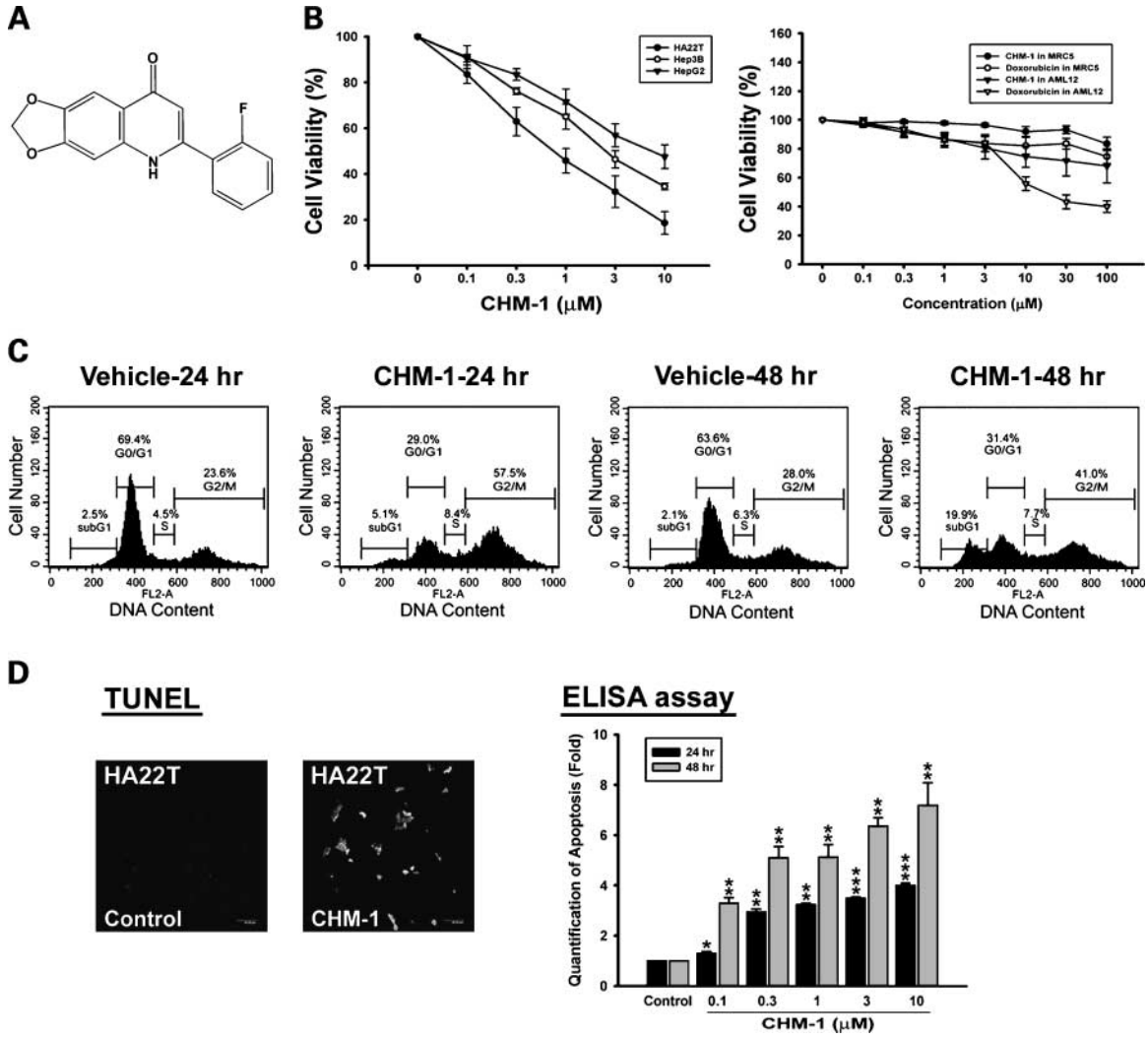

Figure 1. Effect of CHM-1 on cell growth and cell cycle progression in human hepatocellular carcinoma cells. **A,** chemical structure of CHM-1. **B,** HA22T, Hep3B, and HepG2 cells were treated with the indicated concentrations of CHM-1 for 24 h (*left*). MRC5 and AML12 cells were cultured for 24 h in the presence of CHM-1 or doxorubicin (0-100 μmol/L; *right*). Then, the cell viability was determined using MTT assay. **C,** time effect of CHM-1 on cell cycle distribution. HA22T cells were treated with vehicle (DMSO) or CHM-1 (1 μmol/L) for the indicated times. **D,** after 24-h treatment with vehicle or CHM-1 (1 μmol/L), terminal deoxynucleotidyl transferase–mediated dUTP nick end labeling assay was used to detect apoptotic effect (*left*). Then, HA22T cells were treated with indicated concentrations of CHM-1 to determine apoptosis using Cell Death ELISA^{PLUS} kit (*right*). Mean ± SE of five independent experiments. *, $P < 0.05$; **, $P < 0.01$; ***, $P < 0.001$, compared with the respective control group.

CHM-1 Induces Change in Expressed and Phosphorylated Status of G_2-M Regulators in Human Hepatocellular Carcinoma Cells

As shown in Fig. 3A, CHM-1 did not change the levels of cyclin A, but the expression of cyclin B1 was sustained at high levels in CHM-1-treated cells. There was no difference in total Cdc2 and Tyr^{15}-phosphorylated Cdc2 expression after CHM-1 treatment. Nonetheless, phosphorylation at the Thr^{161} site of Cdc2 was increased after CHM-1 treatment at the indicated times. Furthermore, CHM-1 significantly increased the binding of cyclin B1 to Cdc2 in HA22T cells (Fig. 3B). The Cdc2 kinase activity was low in control cells and was substantially increased in cells treated with CHM-1, similar to that of paclitaxel (Fig. 3C, *left*). Moreover, we found that treating the cells with CHM-1 together with roscovitine, a specific cyclin-dependent kinase inhibitor, significantly abolished CHM-1-induced Cdc2 activity and growth inhibition (Fig. 3C, *right*). Next, we examined the status of phosphorylated polypeptides found only in mitotic cells using MPM2 antibody. After 24 h of treatment, CHM-1 induced a concentration-dependent elevation in MPM2 phosphoepitopes, and CHM-1-induced effects were prevented by cotreatment with roscovitine (Fig. 3D).

CHM-1 Induces a Caspase-Independent Manner in Human Hepatocellular Carcinoma Cells

As shown in Fig. 4A, CHM-1 did not induce the activation of effector caspases (caspase-3, caspase-6, and caspase-7) or initiator caspases (caspase-8 and caspase-9) in HA22T cells.

After treatment for 12 and 24 h, the levels of cIAP1, cIAP2, XIAP, and survivin were not altered in CHM-1-treated cells (Fig. 4B). CHM-1 also did not increase the activity of caspase-3, caspase-8, or caspase-9 after a 24-h application (Fig. 4C). Staurosporine was used as a positive control for the cleavage and activation of caspases. Moreover, z-VAD-fmk, a general inhibitor of caspases, did not inhibit CHM-1-induced growth inhibition in HA22T cells (Fig. 4D).

CHM-1 Induces AIF Translocation and AIF siRNA Prevents CHM-1-Induced AIF Translocation in Human Hepatocellular Carcinoma Cells

Subcellular fraction showed that treatment of cells with CHM-1 dramatically redistributed AIF, but not endonuclease G, from the mitochondria to the cytosol, subsequent to the nucleus (Fig. 5A). Analysis by confocal microscopy revealed that AIF was translocated into the nucleus and caused nuclear condensation after 24-h treatment with CHM-1 (Fig. 5B). As shown in Fig. 5C, both CHM-1 and roscovitine induced AIF release in the cytosolic fraction, and cotreatment with roscovitine did not prevent CHM-1-induced AIF translocation. We next showed that the AIF protein level was greatly reduced at 24 h after treatment with AIF siRNA but not after treatment with control siRNA (Fig. 5D, *top*). Moreover, siRNA targeting of the AIF substantially attenuated CHM-1-induced AIF translocation to the cytosol (Fig. 5D, *bottom*). Thus, this RNA interference

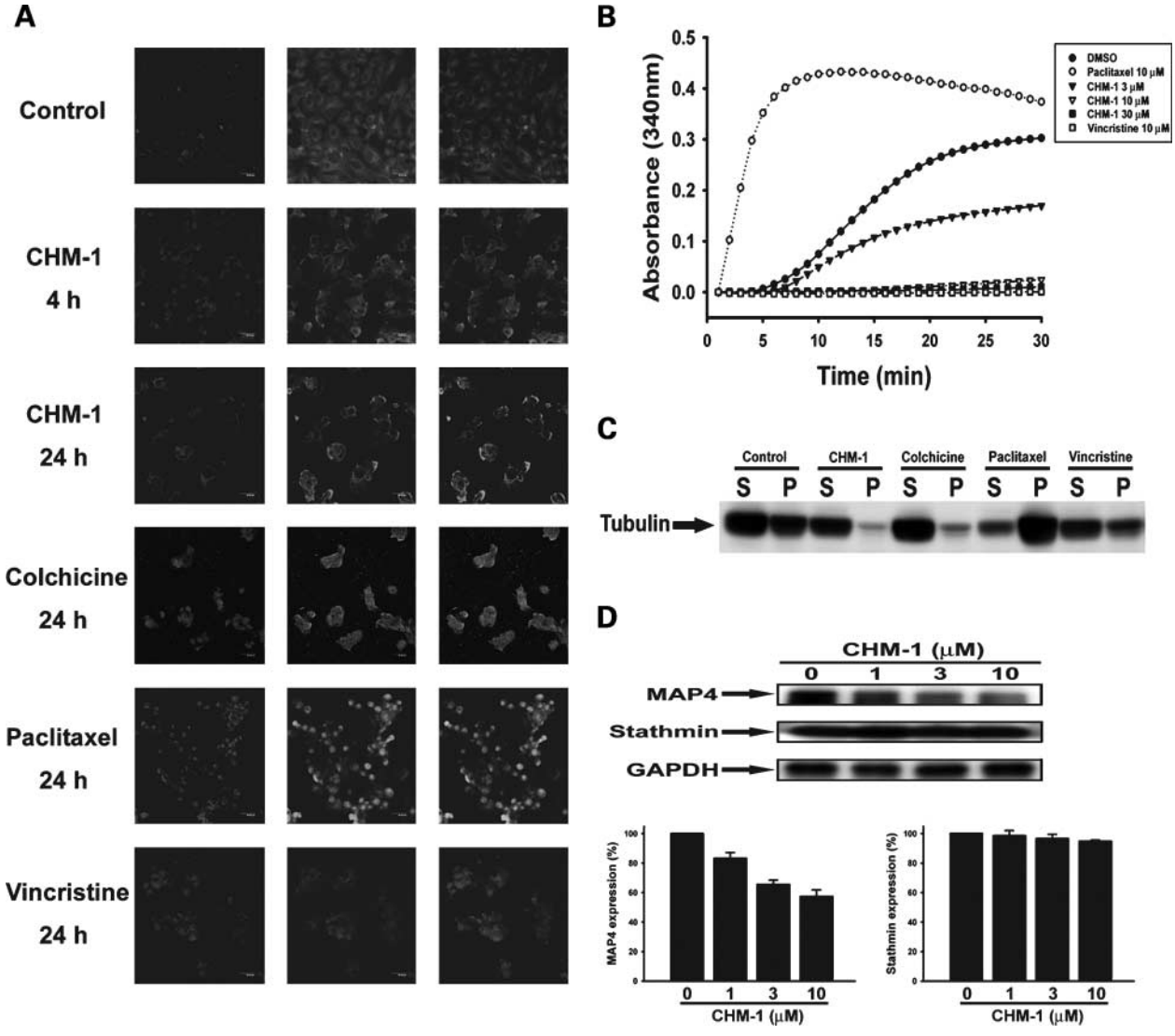

Figure 2. Effect of CHM-1 on microtubule assembly *in vitro* and *in vivo*. **A,** cells were incubated with vehicle (DMSO) or 3 μmol/L CHM-1 for 4 h and treated with 3 μmol/L CHM-1, 3 μmol/L colchicine, 3 μmol/L paclitaxel, or 3 μmol/L vincristine for 24 h. *Left,* 4′,6-diamidino-2-phenylindole; *middle,* microtubule network; *right,* merged microtubule network and 4′,6-diamidino-2-phenylindole. **B,** tubulin proteins (>99% purity) were suspended in G-PEM buffer plus glycerol in the absence (DMSO) or presence of 3, 10, or 30 μmol/L CHM-1, 10 μmol/L paclitaxel, or 10 μmol/L vincristine. **C,** after 24-h treatment with vehicle or 3 μmol/L antimitotic agents, cytosolic (*S,* soluble) and cytoskeletal (*P,* polymerized tubulin) tubulin fractions were separated and followed by immunoblotting with antibody against β-tubulin. **D,** after 24-h treatment with vehicle or CHM-1, HA22T cells were harvested and lysed for the detection of MAP4, stathmin, and GAPDH protein expression.

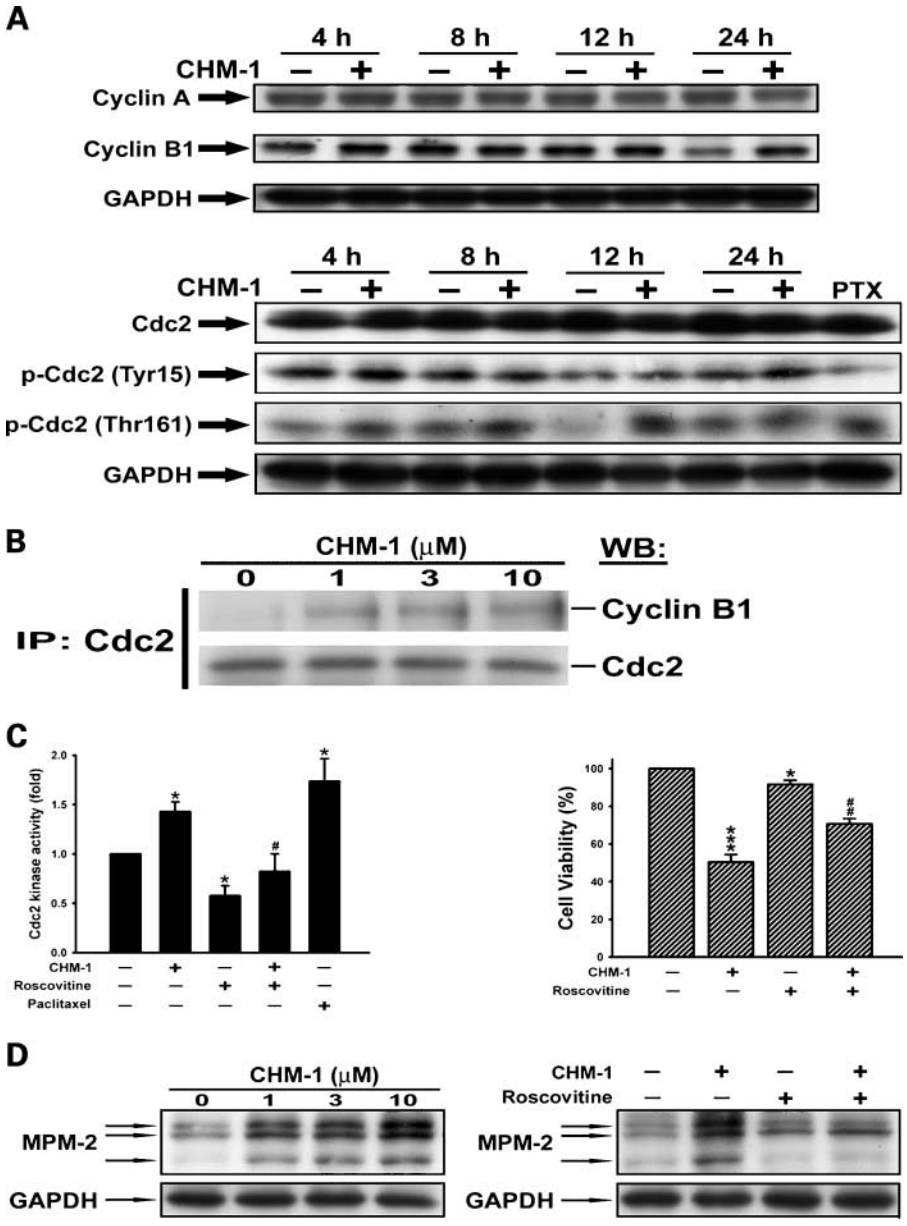

Figure 3. Effect of CHM-1 on G_2-M cell cycle regulatory proteins and kinase activity. **A,** HA22T cells were treated with vehicle (DMSO), CHM-1 (3 μmol/L), or paclitaxel (PTX, 3 μmol/L) for the indicated time. Cells were then harvested and lysed for the detection of cyclin A, cyclin B1, Cdc2, phospho-Tyr^{15}-Cdc2, phospho-Thr^{161}-Cdc2, and GAPDH protein expression. **B,** total cell lysates from cells treated with CHM-1 (0-10 μmol/L) for 24 h were used to immunoprecipitate Cdc2 complexes. Then, Western blots were done to determine the association of cyclin B1 with immunoprecipitated Cdc2 complexes. **C,** HA22T cells were treated DMSO (as control), paclitaxel (3 μmol/L), or CHM-1 (3 μmol/L) for 24 h in the absence or presence of roscovitine (10 μmol/L). Then, Cdc2 was immunoprecipitated by anti-Cdc2 antibody and mixed with protein A/G^{PLUS}-agarose beads. The Cdc2 kinase activity was measured by [γ-^{32}P]ATP incorporation into the substrate histone H1 (*left*). HA22T cells were incubated in 1 μmol/L CHM-1 with or without roscovitine (10 μmol/L) for 24 h. Then, the cell viability was determined using MTT assay (*right*). Mean ± SE of four independent experiments. *, $P < 0.05$; ***, $P < 0.001$, compared with the respective control group; #, $P < 0.05$; ##, $P < 0.01$; ###, $P < 0.001$, compared with CHM-1-treated group. **D,** HA22T cells were incubated in the indicated concentrations of CHM-1 with or without roscovitine (10 μmol/L) for 24 h. Cells were then harvested and lysed for the detection of MPM2 and GAPDH protein expression.

further confirms that the mitochondrial-nuclear translocation of AIF is indeed the target of CHM-1 treatment.

In vivo Antitumor Activity of CHM-1

To investigate the *in vivo* antitumor activity of CHM-1, we carried out xenografts with HA22T cells in athymic severe combined immunodeficient mice. As shown in Fig. 6A, CHM-1 induced a dose-dependent inhibition of HA22T tumor growth (10 mg/kg CHM-1, 128 ± 26 mm^3, $P < 0.01$ versus vehicle; vehicle-treated group = 491 ± 83 mm^3 on day 70). In line with the tumor growth suppression

results, CHM-1 prolonged the lifespan of the HA22T-bearing mice (Fig. 6B). CHM-1 showed significant antitumor activity, with a T/C value of 167% ($P < 0.01$). In comparison, doxorubicin conferred no antitumor benefit and the doxorubicin-treated mice all died on day 53 possibly due to the toxicity of the drug. Moreover, in these two animal models, body weights were not significantly affected by CHM-1. In support of the antitumor mechanism in CHM-1-treated cells, we next examined the immunohistochemical AIF and MPM2 protein expression using tumor specimens from control and CHM-1-treated animals. The distribution of AIF was almost detected in the cytosol in the vehicle-treated group, but the translocation of AIF and accumulation of MPM2 in nuclei of apoptotic cells increased significantly in tissue treated with CHM-1 (Fig. 6C).

Discussion

In this study, CHM-1 exhibited promising antitumor actions against human hepatocellular carcinoma cells. CHM-1 induced a significant concentration-dependent growth inhibition and apoptosis in hepatocellular carcinoma cells. CHM-1 produced a dose-dependent tumor regression and prolonged the lifespan of mice carrying liver cancer xenografts, indicating its *in vivo* efficacy. We also compared the influence of CHM-1 with that of doxorubicin in hepatocellular carcinoma and normal cells. The range of IC_{50} values between hepatocellular carcinoma cells and normal cells were broader for CHM-1 than for doxorubicin. In the *in vivo* model, the antitumor activity of CHM-1 was found to be equal and even superior to doxorubicin; importantly, body weight was not significantly affected by CHM-1 compared with doxorubicin. Therefore, we suggest that CHM-1 could be a more efficacious and safe anticancer agent for treatment of human hepatocellular carcinomas.

In previous studies, we showed 2-phenyl-4-quinolone derivatives, including CHM-1, interacted with tubulin at colchicine-binding site and inhibited tubulin polymerization with IC_{50} values equivalent to those obtained with podophyllotoxin and combretastatin A-4 (11–15). Consistent with these biochemical effects, in intact cells, CHM-1 disrupted the intracellular microtubule network and caused inhibition of the microtubule assembly. Numerous proteins and kinases that interact with microtubules and/or free tubulin dimmer also have the potential to regulate both catastrophe and rescue rates (22). The overexpression/activation of stathmin and/or the down-regulation/inactivation of MAP4 should increase the dynamicity and decrease the stability of microtubules. In our study, the expression of MAP4 was inhibited by CHM-1 in HA22T cells. This suggests that the down-regulation of MAP4 may be involved in CHM-1-induced inhibition of tubulin polymerization.

To allow cells to progress from the G_2 to the M phase, the Cdc2/cyclin B1 complex is active (23), meaning that Cdc2

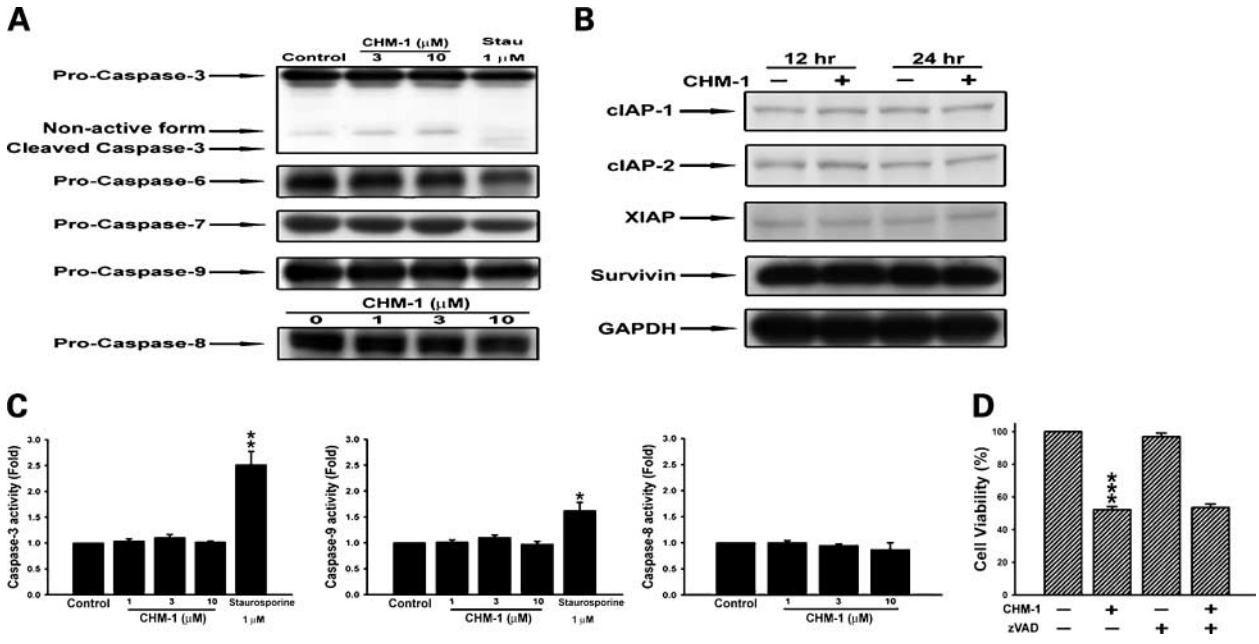

Figure 4. Effect of CHM-1 on caspase cascade and inhibitor of apoptosis proteins in human hepatocellular carcinoma cells. **A,** HA22T cells were treated with DMSO (as control), the indicated concentrations of CHM-1, or staurosporine (*Stau*; 1 μmol/L) for 24 h. Cell extracts were then subjected to Western blotting using anti-caspase-3, anti-caspase-6, anti-caspase-7, anti-caspase-8, and anti-caspase-9 antibodies. **B,** HA22T cells were incubated in the absence or presence of CHM-1 (3 μmol/L) for the indicated time. Cells were lysed for the detection of cIAP1, cIAP2, XIAP, survivin, and GAPDH protein expression. **C,** caspase protease activity in HA22T cell lysates were assayed by spectrophometric detection. **D,** HA22T cells were incubated in 1 μmol/L CHM-1 with or without z-VAD-fmk (50 μmol/L) for 24 h. Then, the cell viability was determined using MTT assay. Mean ± SE of five independent experiments. *, $P < 0.05$; **, $P < 0.01$; ***, $P < 0.001$, compared with the respective control group.

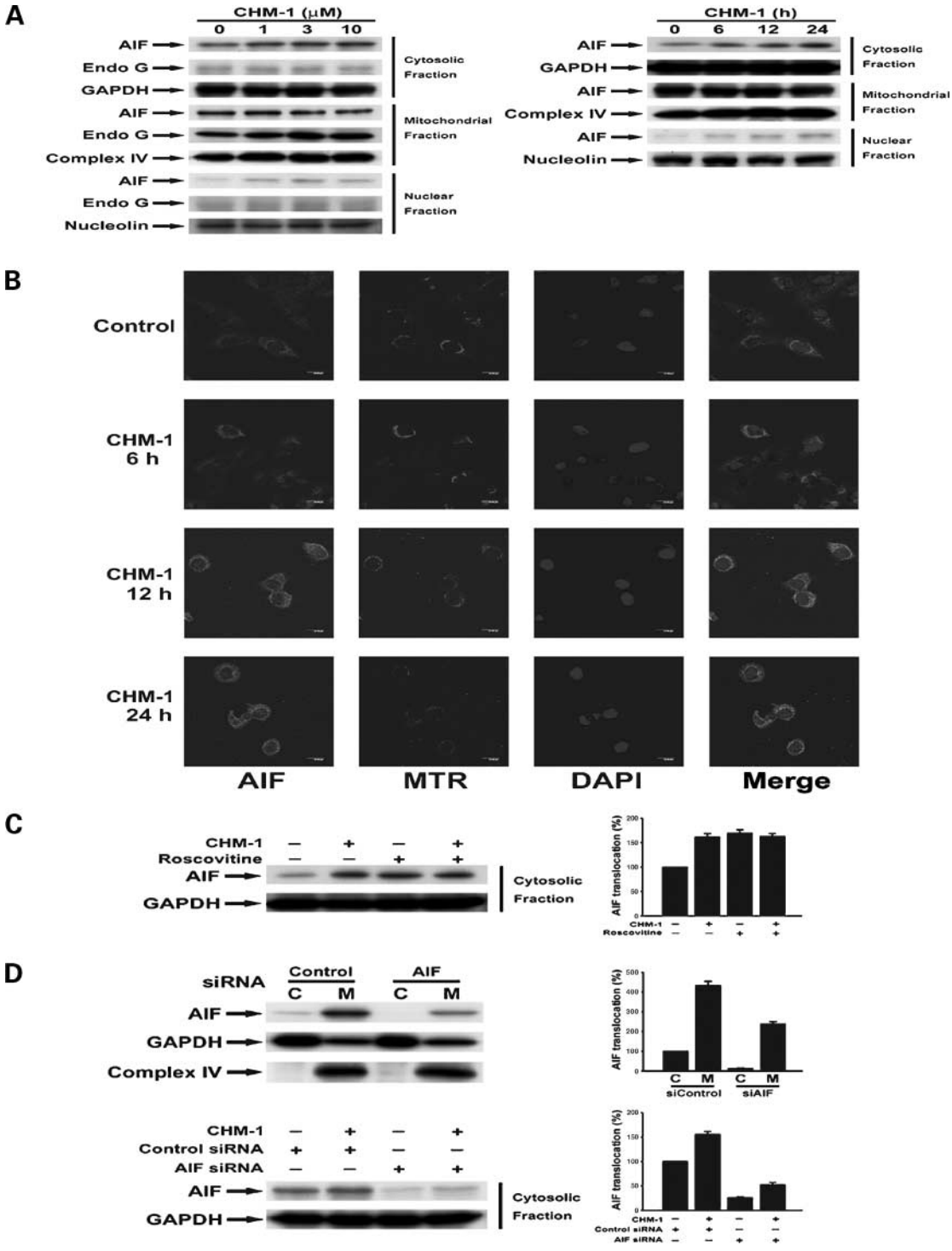

Figure 5. Effect of CHM-1 on AIF translocation in AIF siRNA-transfected human hepatocellular carcinoma cells. **A,** analysis of AIF and endonuclease G translocation by subcellular fractionation. HA22T cells were treated with the indicated concentrations of CHM-1 for 24 h (*left*). HA22T cells were incubated in the absence or presence of CHM-1 (3 μmol/L) for the indicated time (*right*). GAPDH, complex IV, and nucleolin were used as cytosolic, mitochondrial, and nuclear marker proteins, respectively. **B,** HA22T cells were treated with DMSO (as control) and CHM-1 (3 μmol/L) for the indicated time. After incubation, imaging was analyzed by the confocal microscope. **C,** HA22T cells were incubated in CHM-1 (3 μmol/L) with or without roscovitine (10 μmol/L) for 24 h. Cells were then harvested and lysed for the detection of AIF protein expression in cytosol fraction by Western blot analysis. **D,** HA22T cells were transfected with 200 nmol/L AIF siRNA or control siRNA followed by Western blot analysis of the cytosolic and mitochondrial fractions (*top*). Analysis of AIF translocation by cytosolic fraction in AIF siRNA or control siRNA-transfected HA22T cells after 24-h treatment with CHM-1 (3 μmol/L; *bottom*). Representative of four independent experiments.

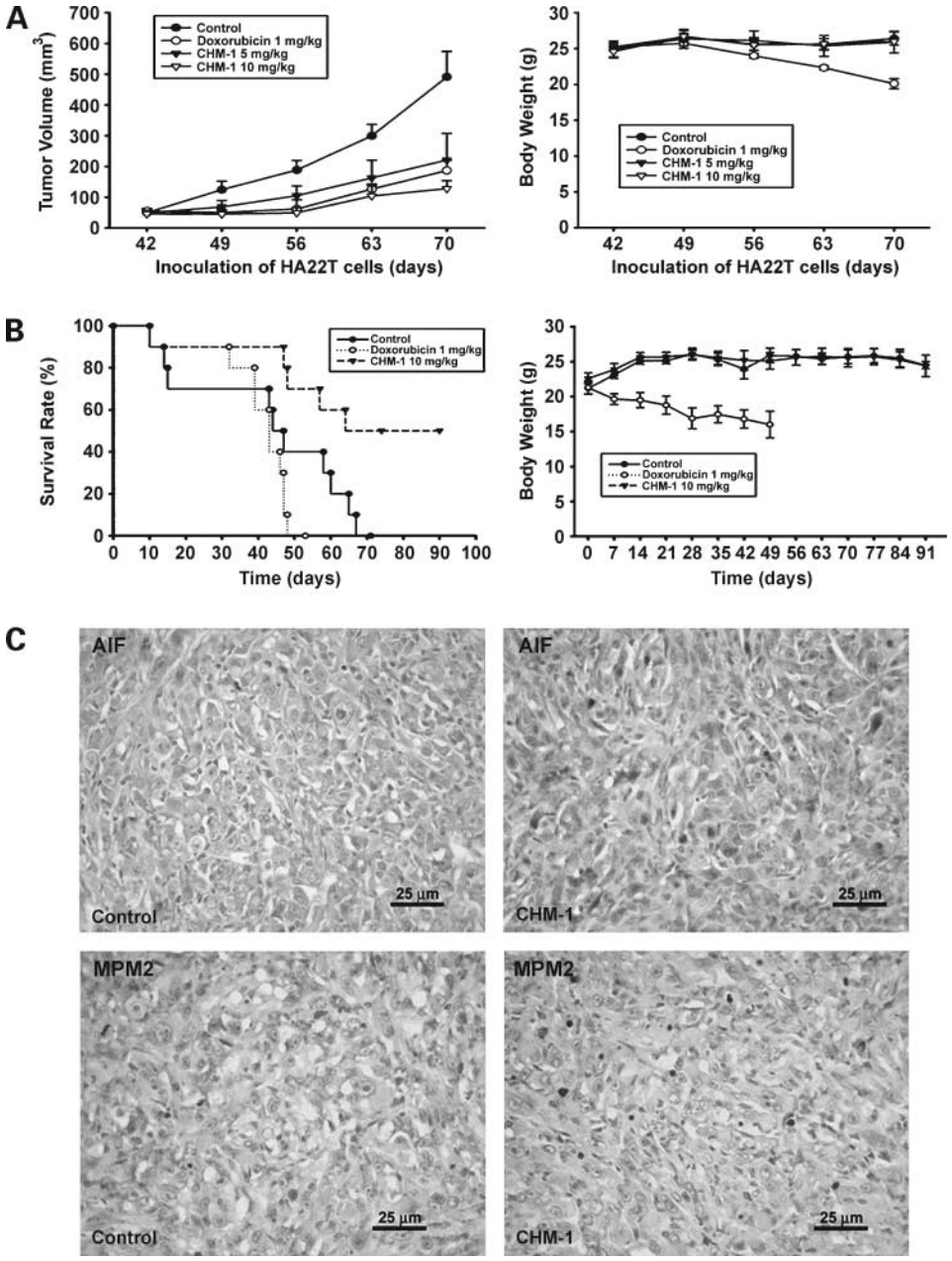

Figure 6. Effect of CHM-1 on antitumor activity and the expression of AIF and MPM2 *in vivo*. **A,** HA22T cells were used to establish xenografts in severe combined immunodeficient mice, and tumor-bearing animals were treated on day 42. Animals (7 mice/group) were given vehicle (control), CHM-1 (5 and 10 mg/kg), or doxorubicin (1 mg/kg) by i.p. injection. HA22T tumor samples from animals were obtained and weighted at the end of treatment (day 70). Body weights of mice were determined every week. **B,** HA22T cells were injected i.p. into severe combined immunodeficient mice. Animals (10 mice/group) were given vehicle (control), CHM-1, and doxorubicin (1 day after tumor cell inoculation) by i.p. injection twice weekly for 7 consecutive weeks. **C,** protein expression of AIF and MPM2 was examined using immunohistochemical analyses in HA22T tumor samples. Representative of four independent experiments.

has undergone an activating phosphorylation (on Thr^{161}) by CAK, that inhibitory phosphorylation (on Thr^{14} and Tyr^{15}) has been removed by active Cdc25C phosphatase, that Cdc2 associates with cyclin B1, and that complex translocates to the nucleus (24). In this study, CHM-1 arrested the growth of cancer cells at the G_2-M phase and then induced apoptotic cell death. CHM-1 significantly increased the protein level of cyclin B1, Thr^{161}-phosphorylated Cdc2, but had no effect on the expression of Tyr^{15}-phosphorylated Cdc2 and total Cdc2. The kinase assay revealed that CHM-1 activated Cdc2 kinase activity, and the formation of Cdc2/cyclin B1 complex was increased by CHM-1. The pattern of CHM-1-induced activation of cyclin B1 and Cdc2 kinase activity is consistent with the effects of

the antimitotic agents (25, 26). In addition, the CHM-1-induced activation of Cdc2 kinase activity, the elevation of MPM2 phosphoepitopes, and the inhibition of cell growth were all attenuated by roscovitine. Taken together, we show that in addition to directly disrupting microtubules CHM-1 induces mitotic arrest by increasing the activation of Cdc2/cyclin B1 complex activity.

Caspases exist as inactive zymogens in normal and surviving cells and perform proteolytic processing on activation during apoptosis. Members of the inhibitor of apoptosis protein family counteract both the activation and the activity of caspases (27). In the present study, neither initiator caspases nor effector caspases were activated by CHM-1. Furthermore, the general caspase inhibitor z-VAD-fmk could not prevent CHM-1-induced cell death. Therefore, CHM-1 appears to induce apoptosis via a caspase-independent mechanism in human hepatocellular carcinoma cells. Recent studies suggest that caspase activation is not the sole pathway to induce apoptotic cell death (28). Mitochondria can release factors involved in caspase-independent cell death, including AIF and endonuclease G. AIF is ubiquitously expressed both in normal tissues and in a variety of cancer cell lines and is found to be localized in mitochondria-rich areas (29). Herein, our data showed that CHM-1 induced AIF translocation and nuclear condensation in HA22T cells. CHM-1-induced AIF translocation was not attenuated by roscovitine, and roscovitine alone would trigger AIF release in cytosol. This roscovitine-induced event was also observed in U937 cells (30). Moreover, siRNA knockdown of the AIF protein in HA22T cells effectively attenuated CHM-1-induced AIF translocation. In immunohistochemical analyses, we found that CHM-1 significantly increased AIF translocation in nuclei in HA22T tumor tissues. These findings suggest that AIF-dependent pathway plays a pivotal role in CHM-1-induced apoptosis in human hepatocellular carcinoma cells.

Caspase-independent cell death pathways are important safeguard mechanisms to protect the organism against unwanted and potential harmful cells when caspase-mediated routes fail but can also be triggered in response to cytotoxic agents or other death stimuli (31). The major challenge in treating cancer is that many tumor cells carry mutations in key apoptotic genes, such as p53, Bcl-2 family proteins, or those affecting caspase signaling, thus making treatment with traditional chemotherapeutic agents ineffective (32). The triggering of caspase-independent processes, therefore, has become an alternative approach to eradicate tumor cells (33, 34). Accordingly, the capability of inducing cell death even in the absence of the caspase cascade may be a key feature of CHM-1 and explains its efficiency to trigger cell death in a variety of drug-resistant cell types including, in particular, tumor cells with defects in caspase activation.

In this study, we show that CHM-1 induces mitotic arrest and apoptosis by binding to tubulin and inhibiting tubulin polymerization. CHM-1 causes mitotic arrest, at least partly, by modulating Cdc2/cyclin B1 complex activity and then apoptosis executed by a caspase-independent pathway. Additional studies on the pharmacokinetic properties of CHM-1, including absorption, distribution, metabolism, excretion, and toxicity, are needed to proceed in the future. We suggest that CHM-1 deserves further investigation and has the potential to replace doxorubicin, which is used in the systemic chemotherapy or transarterial chemoembolization for patients with hepatocellular carcinoma.

References

1. Bosch FX, Ribes J, Diaz M, Cleries R. Primary liver cancer: worldwide incidence and trends. Gastroenterology 2004;127:S5 – 16.

2. Yu MW, Chang HC, Liaw YF, et al. Familial risk of hepatocellular carcinoma among chronic hepatitis B carriers and their relatives. J Natl Cancer Inst 2000;92:1159 – 64.

3. El-Serag HB. Hepatocellular carcinoma: recent trends in the United States. Gastroenterology 2004;127:S27 – 34.

4. Burroughs A, Hochhauser D, Meyer T. Systemic treatment and liver transplantation for hepatocellular carcinoma: two ends of the therapeutic spectrum. Lancet Oncol 2004;5:409 – 18.

5. Huang CC, Wu MC, Xu GW, et al. Overexpression of the MDR1 gene and P-glycoprotein in human hepatocellular carcinoma. J Natl Cancer Inst 1992;84:262 – 4.

6. Bruix J, Sherman M, Llovet JM, et al. Clinical management of hepatocellular carcinoma. Conclusions of the Barcelona-2000 EASL conference. European Association for the Study of the Liver. J Hepatol 2001;35:421 – 30.

7. Jordan MA, Wilson L. Microtubules as a target for anticancer drugs. Nat Rev Cancer 2004;4:253 – 65.

8. Bhalla KN. Microtubule-targeted anticancer agents and apoptosis. Oncogene 2003;22:9075 – 86.

9. Giannakakou P, Sackett D, Fojo T. Tubulin/microtubules: still a promising target for new chemotherapeutic agents. J Natl Cancer Inst 2000;92:182 – 3.

10. Hooper DC. Mode of action of fluoroquinolones. Drugs 1999;58 Suppl 2:6 – 10.

11. Kuo SC, Lee HZ, Juang JP, et al. Synthesis and cytotoxicity of 1,6,7,8-substituted 2-(4′-substituted phenyl)-4-quinolones and related compounds: identification as antimitotic agents interacting with tubulin. J Med Chem 1993;36:1146 – 56.

12. Li L, Wang HK, Kuo SC, et al. Antitumor agents. 150. 2′,3′,4′,5′,5,6,7-Substituted 2-phenyl-4-quinolones and related compounds: their synthesis, cytotoxicity, and inhibition of tubulin polymerization. J Med Chem 1994;37:1126 – 35.

13. Xia Y, Yang ZY, Xia P, et al. Antitumor agents. 181. Synthesis and biological evaluation of 6,7,2′,3′,4′-substituted-1,2,3,4-tetrahydro-2-phenyl-4-quinolones as a new class of antimitotic antitumor agents. J Med Chem 1998;41:1155 – 62.

14. Xia Y, Yang ZY, Xia P, et al. Antitumor agents. 211. Fluorinated 2-phenyl-4-quinolone derivatives as antimitotic antitumor agents. J Med Chem 2001;44:3932 – 6.

15. Chen YC, Lu PH, Pan SL, et al. Quinolone analogue inhibits tubulin polymerization and induces apoptosis via Cdk1-involved signaling pathways. Biochem Pharmacol 2007;74:10 – 9.

16. Huang LJ, Hsieh MC, Teng CM, Lee KH, Kuo SC. Synthesis and antiplatelet activity of phenyl quinolones. Bioorg Med Chem 1998;6: 1657 – 62.

17. Ferlin MG, Chiarelotto G, Gasparotto V, et al. Synthesis and *in vitro* and *in vivo* antitumor activity of 2-phenylpyrroloquinolin-4-ones. J Med Chem 2005;48:3417 – 27.

18. Wang SW, Pan SL, Peng CY, et al. CHM-1 inhibits hepatocyte growth factor-induced invasion of SK-Hep-1 human hepatocellular carcinoma cells by suppressing matrix metalloproteinase-9 expression. Cancer Lett 2007; 257:87 – 96.

19. Pan SL, Guh JH, Peng CY, et al. YC-1 [3-(5′-hydroxymethyl-2′-furyl)-1-benzyl indazole] inhibits endothelial cell functions induced by angiogenic factors *in vitro* and angiogenesis *in vivo* models. J Pharmacol Exp Ther 2005;314:35 – 42.

20. Wang SW, Pan SL, Guh JH, et al. YC-1 [3-(5′-hydroxymethyl-2′-furyl)-1-benzyl Indazole] exhibits a novel antiproliferative effect and arrests the cell cycle in G_{0-1} in human hepatocellular carcinoma cells. J Pharmacol Exp Ther 2005;312:917 – 25.

21. Nogales E. Structural insights into microtubule function. Annu Rev Biochem 2000;69:277 – 302.

22. Schmit TL, Ahmad N. Regulation of mitosis via mitotic kinases: new opportunities for cancer management. Mol Cancer Ther 2007;6: 1920 – 31.

23. Morgan DO. Principles of CDK regulation. Nature 1995;374:131 – 4.

24. Coleman TR, Dunphy WG. Cdc2 regulatory factors. Curr Opin Cell Biol 1994;6:877 – 82.

25. Donaldson KL, Goolsby GL, Kiener PA, Wahl AF. Activation of p34cdc2 coincident with taxol-induced apoptosis. Cell Growth Differ 1994;5:1041 – 50.

26. Huang YT, Huang DM, Guh JH, Chen IL, Tzeng CC, Teng CM. CIL-102 interacts with microtubule polymerization and causes mitotic arrest following apoptosis in the human prostate cancer PC-3 cell line. J Biol Chem 2005;280:2771 – 9.

27. Riedl SJ, Shi Y. Molecular mechanisms of caspase regulation during apoptosis. Nat Rev Mol Cell Biol 2004;5:897 – 907.

28. Broker LE, Kruyt FA, Giaccone G. Cell death independent of caspases: a review. Clin Cancer Res 2005;11:3155 – 62.

29. Daugas E, Nochy D, Ravagnan L, et al. Apoptosis-inducing factor (AIF): a ubiquitous mitochondrial oxidoreductase involved in apoptosis. FEBS Lett 2000;476:118 – 23.

30. Yu C, Rahmani M, Dai Y, et al. The lethal effects of pharmacological cyclin-dependent kinase inhibitors in human leukemia cells proceed through a phosphatidylinositol 3-kinase/Akt-dependent process. Cancer Res 2003;63:1822 – 33.

31. Cregan SP, Dawson VL, Slack RS. Role of AIF in caspase-dependent and caspase-independent cell death. Oncogene 2004;23:2785 – 96.

32. Johnstone RW, Ruefli AA, Lowe SW. Apoptosis: a link between cancer genetics and chemotherapy. Cell 2002;108:153 – 64.

33. Kang YH, Yi MJ, Kim MJ, et al. Caspase-independent cell death by arsenic trioxide in human cervical cancer cells: reactive oxygen species-mediated poly(ADP-ribose) polymerase-1 activation signals apoptosis-inducing factor release from mitochondria. Cancer Res 2004;64:8960 – 7.

34. Ishitsuka K, Hideshima T, Hamasaki M, et al. Novel inosine monophosphate dehydrogenase inhibitor VX-944 induces apoptosis in multiple myeloma cells primarily via caspase-independent AIF/Endo G pathway. Oncogene 2005;24:5888 – 96.